

# Solvation Structure around the $\text{Li}^+$ Ion in Mixed Cyclic/Linear Carbonate Solutions Unveiled by the Raman Noncoincidence Effect

Maria Grazia Giorgini,<sup>\*,†</sup> Kazuma Futamatagawa,<sup>‡</sup> Hajime Torii,<sup>\*,‡,§</sup> Maurizio Musso,<sup>||</sup> and Stefano Cerini<sup>†</sup>

<sup>†</sup>Department of Industrial Chemistry "Toso Montanari", University of Bologna, Viale del Risorgimento 4, I-40136 Bologna, Italy

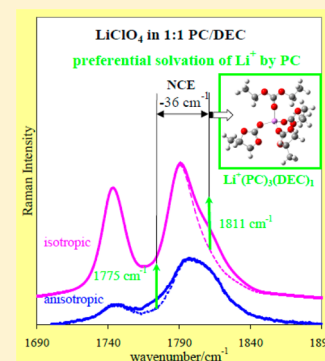
<sup>‡</sup>Department of Chemistry, Faculty of Education, Shizuoka University, 836 Ohya, Shizuoka 422-8529, Japan

<sup>§</sup>Department of Optoelectronics and Nanostructure Science, Graduate School of Science and Technology, Shizuoka University, 836 Ohya, Shizuoka 422-8529, Japan

<sup>||</sup>Fachbereich Materialforschung und Physik, Abteilung Physik und Biophysik, Universität Salzburg, Hellbrunnerstraße 34, A-5020 Salzburg, Austria

## S Supporting Information

**ABSTRACT:** The solvation structure around the  $\text{Li}^+$  ion in a mixed cyclic/linear carbonate solution, an important factor for the performance of lithium-based rechargeable batteries, is examined by measuring and analyzing the noncoincidence effect observed for the  $\text{C}=\text{O}$  stretching Raman band. This technique has the advantage of perceiving relative distances and orientations of solvent molecules clustering around an ion in the first solvation shell and, hence, of developing information on the solvation structure along the wavenumber axis rather than along the intensity axis of the spectra. It is shown that, taking the solution of  $\text{Li}^+\text{ClO}_4^-$  in the 1:1 mixed solvent of propylene carbonate (PC) and diethyl carbonate (DEC) as an example case, the  $\text{Li}^+$  ion is preferentially solvated by PC molecules [primarily as  $(\text{PC})_3(\text{DEC})_1\text{Li}^+$ ] and is totally protected from direct interaction (contact ion pairing) with the  $\text{ClO}_4^-$  ion. The solvation structures in neat PC and neat DEC solvents are also discussed.



Ion solvation is a central, and still an open, issue in many chemical, biochemical, and electrochemical processes. One of those important processes would be the functioning of lithium-based rechargeable batteries.<sup>1–3</sup> Their performance depends on the electrode materials and processes on the one hand and on the charge carrier concentration and mobility in the electrolyte solution on the other hand. With regard to the latter, high charge density of the  $\text{Li}^+$  ion should be sufficiently stabilized, and at the same time, the electrolyte solution should have sufficiently high fluidity. A usual practice to make these two factors compatible is to employ a mixed solvent, consisting of a highly dipolar liquid such as a cyclic carbonate stabilizing the high charge density (but highly viscous) and a liquid of lower viscosity such as a linear carbonate (being less dipolar). Quite often ethylene or propylene carbonate (with dielectric constant  $\epsilon = 65\text{--}90$  and viscosity  $\eta \cong 2.5$  cP, abbreviated as EC and PC) is used for the former, and dimethyl, diethyl, or ethyl methyl carbonate (with  $\epsilon \cong 3$  and  $\eta = 0.6\text{--}0.9$  cP, abbreviated as DMC, DEC, and EMC) is used for the latter.

The solvation structure around the  $\text{Li}^+$  ion, especially that of the first solvation shell, has been suggested to be important for the interphase chemistry on the electrodes.<sup>4–6</sup> The use of a mixed solvent introduces a complexity in this. One controversial subject in this regard is the presence/absence of the preferential solvation and (if present) its nature for the  $\text{Li}^+$  ion in a mixed cyclic/linear carbonate solution.<sup>7–19</sup> On the

basis of electrospray ionization mass spectroscopy (ESI-MS),<sup>7,8</sup> it has been suggested that there is a strong preferential solvation for  $\text{Li}^+$  in EC/EMC, with the  $\text{Li}^+(\text{EC})_2$  species as the main ingredient.<sup>7</sup> The same type of preferential solvation (i.e., with a higher population of cyclic carbonate around the ion than in the bulk) has also been suggested in some NMR studies<sup>9–11</sup> but with a much larger total solvation number ( $\geq 6$ ).<sup>9,20</sup> It has been argued that some molecules are possibly stripped off from the solvation shell in the detection process in ESI-MS, while the molecules in both the first and second solvation shells are detected in the NMR measurements.<sup>9</sup> In other words, precise composition of the first solvation shell is experimentally still unclear. Another study suggests that there is no such preferential solvation.<sup>17</sup> The solvation structure around the  $\text{Li}^+$  ion has also been studied via molecular dynamics (MD) simulations, but some of those studies suggest that the  $\text{Li}^+$  ion is preferentially solvated by cyclic carbonate,<sup>12,13</sup> while some others suggest that it is preferentially solvated by linear carbonate.<sup>14,15</sup> Therefore, at present, MD simulations are not conclusive in specifying the properties of the first solvation shell.

Received: July 16, 2015

Accepted: August 7, 2015

Published: August 7, 2015

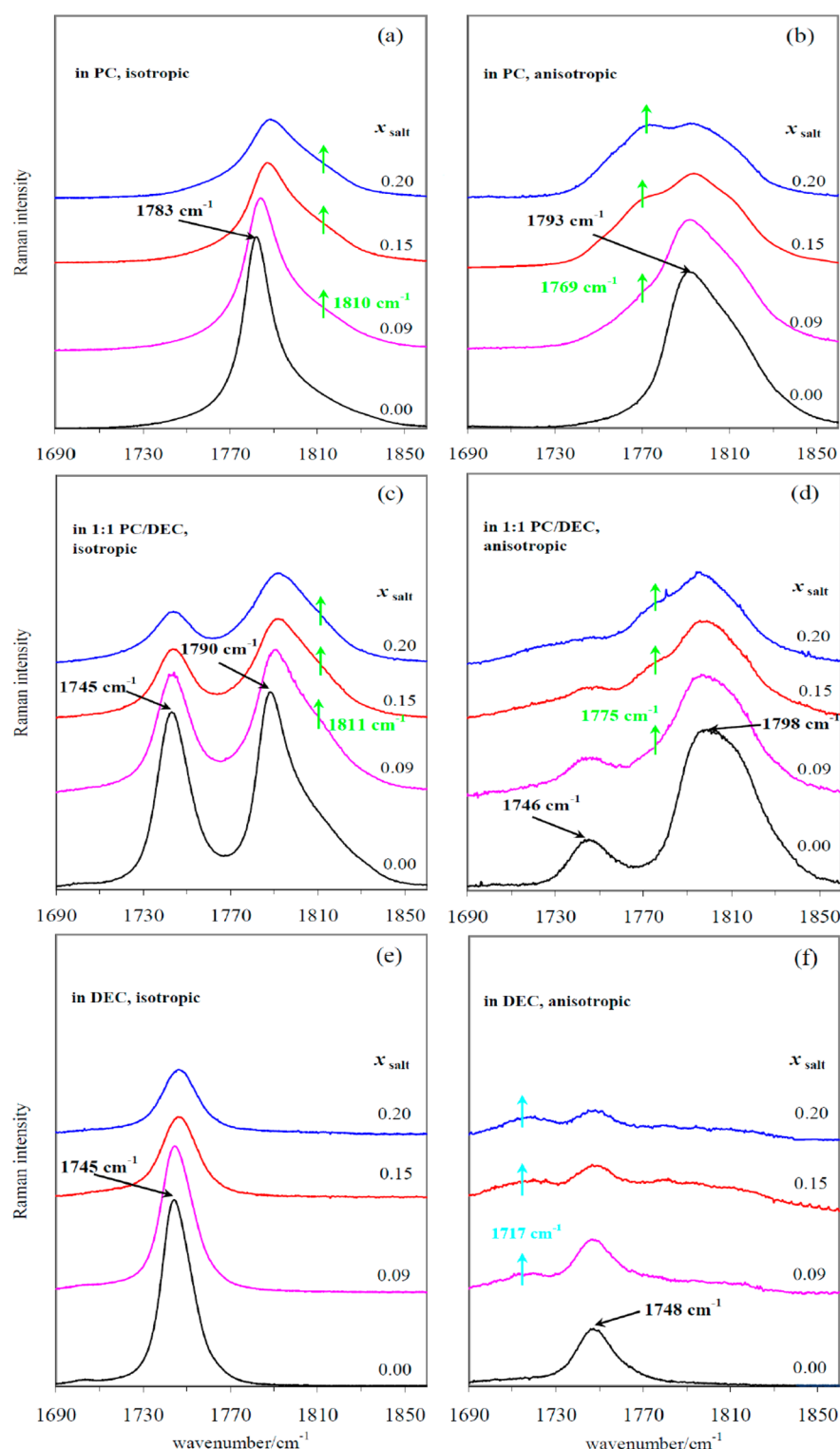


**Figure 1.** (a,c,e) Isotropic and (b,d,f) anisotropic Raman spectra observed in the spectral region around the C=O stretching mode for the solutions of  $\text{LiClO}_4$  in (a,b) liquid PC, (c,d) equimolar PC/DEC liquid mixture, and (e,f) liquid DEC, with mole fractions  $x_{\text{salt}} = 0.00, 0.09, 0.15$ , and  $0.20$  (black, pink, red, and blue, respectively). The intensity scales are adjusted so that the intensities of the bands of the neat liquids ( $x_{\text{salt}} = 0.00$  in panels a, b, e, and f) are shown with the same heights as those of the liquid mixture ( $x_{\text{salt}} = 0.00$  in panels c and d). The light-green and the light-blue vertical arrows indicate the frequency positions of the PC and DEC cluster component bands, respectively. The very weak band appearing at  $\sim 1700 \text{ cm}^{-1}$  in the isotropic Raman spectrum of neat liquid DEC (panel e) arises from the  $^{13}\text{C}=\text{O}$  isotopic impurity.

The purpose of the present study is to solve this problem by measuring and analyzing the noncoincidence effect (NCE) observed for the C=O stretching Raman band. The NCE refers to the phenomenon that the isotropic and anisotropic

components of a polarized Raman band appear at different wavenumber positions (denoted hereafter as  $\tilde{\nu}_{\text{iso}}$  and  $\tilde{\nu}_{\text{aniso}}$ ),<sup>21</sup> and originates from resonant vibrational coupling between molecules.<sup>22–26</sup> The primary mechanism of the resonant

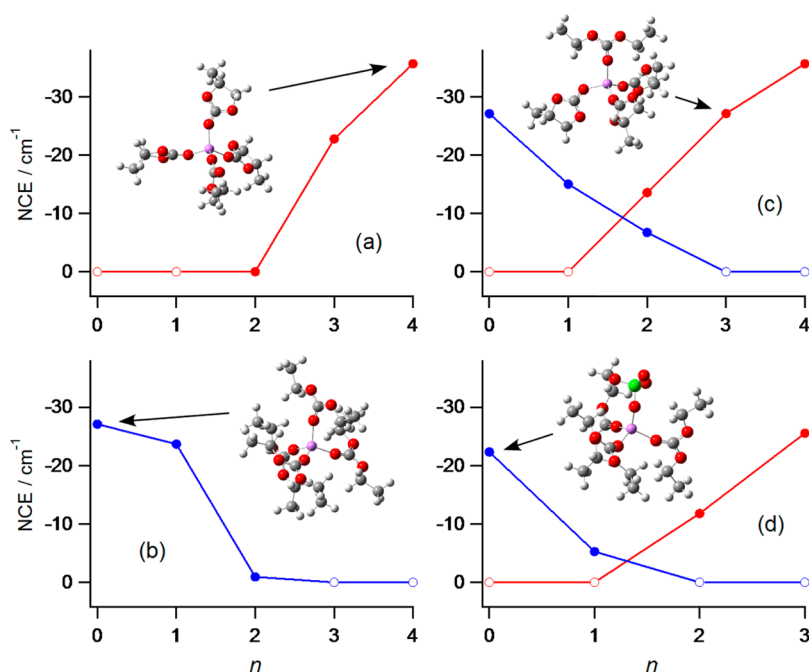


**Figure 2.** NCE values calculated for the C=O stretching bands of PC (in red) and DEC (in blue) of (a)  $(\text{PC})_n\text{Li}^+$  with  $n = 1-4$ , (b)  $(\text{DEC})_{4-n}\text{Li}^+$  with  $n = 0-3$ , (c)  $(\text{PC})_n(\text{DEC})_{4-n}\text{Li}^+$  with  $n = 0-4$ , and (d)  $(\text{PC})_n(\text{DEC})_{3-n}\text{Li}^+\text{ClO}_4^-$  (with  $\text{Li}^+\cdots\text{ClO}_4^-$  contact ion pairing) with  $n = 0-3$  at the B3LYP/6-31+G(2df,p) level. The open circles stand for the points of NCE equal to zero by definition. The filled circles represent calculated nonzero values, although in panels a and b, the value for  $n = 2$  is very close to zero. The structures of  $(\text{PC})_4\text{Li}^+$ ,  $(\text{DEC})_4\text{Li}^+$ ,  $(\text{PC})_3(\text{DEC})_1\text{Li}^+$ , and  $(\text{DEC})_3\text{Li}^+\text{ClO}_4^-$  (whose NCE values are indicated by arrows) are shown in the insets.

vibrational coupling is the transition dipole coupling (TDC),<sup>22–26</sup> and hence the sign and the magnitude of the NCE (defined as  $\tilde{\nu}_{\text{NCE}} \equiv \tilde{\nu}_{\text{aniso}} - \tilde{\nu}_{\text{iso}}$ ) are sensitive to the relative distances and orientations of the interacting molecules. For the C=O stretching Raman bands of the neat liquids of dipolar carbonyl compounds, the NCE is positive and typically large. Our previous studies<sup>27,28</sup> have shown that (1) upon solvation of an alkali or alkaline earth metal salt in liquid acetone a new band appears in the C=O stretching region, and its NCE is large and *negative*, and (2) this large and opposite-sign NCE is reasonably reproduced by calculations of the  $(\text{solvent})_n\text{M}^{m+}$  clusters (where  $\text{M}^{m+}$  denotes the metal ion) with a sufficiently large value of  $n$  ( $n = 4$  for  $\text{Li}^+$ ,  $n = 6$  for  $\text{Na}^+$  and  $\text{Mg}^{2+}$ , and  $n = 6$  or  $8$  for  $\text{Ca}^{2+}$ ,  $\text{Sr}^{2+}$ , and  $\text{Ba}^{2+}$ ) and is interpreted as arising from the resonant vibrational coupling between the molecules clustering around the metal ion. A corollary to this result will be that both the sign and the magnitude of the NCE of such a newly appearing band (called *cluster component band*) are sensitive to the solvation number of the first solvation shell. In other words, information on the solvation number may be developed along the wavenumber axis by the NCE, instead of the intensity axis as in a usual analysis of vibrational spectra,<sup>17,18,29–33</sup> thus avoiding the ambiguity with regard to the relative spectral intensities of the solvated and free species. In the present study we are therefore aiming at clarifying the solvation structure around the  $\text{Li}^+$  ion in a mixed cyclic/linear carbonate solution by utilizing this spectral feature, taking the case of the solution of  $\text{LiClO}_4$  in PC/DEC as an example. Because the C=O stretching bands of cyclic and linear carbonates are somewhat separated in wavenumber (see later), we can observe each of these species separately, leading to discussion on the composition of the first solvation shell.

Polarized Raman spectral measurements were carried out in the wavenumber region 1690–1890  $\text{cm}^{-1}$  around the C=O

stretching mode (the detector pixel separation amounting to  $\sim 0.35 \text{ cm}^{-1}$ ) (i) for the neat liquids of PC and DEC, (ii) for an equimolar (1:1 in mole ratio) PC/DEC liquid mixture, and (iii) for the solutions of  $\text{LiClO}_4$  in these liquids with mole fractions  $x_{\text{salt}} = 0.09, 0.15$ , and  $0.20$ . From the VV and VH spectral profiles measured with the vertically (V) polarized exciting light and the vertically (V) and horizontally (H) polarized scattered light, the isotropic components were derived as  $I_{\text{iso}} = I_{\text{VV}} - (4/3) I_{\text{VH}}$  and the anisotropic ones as  $I_{\text{aniso}} = I_{\text{VH}}$ . Band decomposition of the measured spectral profiles (into the bulk and cluster component bands, simultaneously separating the Fermi resonance band) was carried out by using the GRAMS AI software. To support the discussion on the solvation structure, including the possibility of contact ion pairing between  $\text{Li}^+$  and  $\text{ClO}_4^-$ , we also did spectral measurements in the wavenumber region 880–1000  $\text{cm}^{-1}$  around the Cl–O symmetric stretching mode of the  $\text{ClO}_4^-$  ion and the OCO bending mode of DEC. Calculations of the cluster species were carried out for (i)  $(\text{PC})_n\text{Li}^+$  with  $n = 1-4$ , (ii)  $(\text{DEC})_{4-n}\text{Li}^+$  with  $n = 0-3$ , (iii)  $(\text{PC})_n(\text{DEC})_{4-n}\text{Li}^+$  with  $n = 1-3$ , and (iv)  $(\text{PC})_n(\text{DEC})_{3-n}\text{Li}^+\text{ClO}_4^-$  (with  $\text{Li}^+\cdots\text{ClO}_4^-$  contact ion pairing) with  $n = 0-3$  by density functional theory (DFT) at the B3LYP/6-31+G(2df,p) level using the Gaussian 03 program.<sup>34</sup> The details of the experimental and computational procedures are described in the [Supporting Information](#).

The observed isotropic and anisotropic Raman spectra in the spectral region of the C=O stretching mode are shown in [Figure 1](#). Inspecting first the spectra of the neat liquids and the equimolar binary mixture ( $x_{\text{salt}} = 0.00$ ), the following three features are recognized: (1) for neat PC the NCE is large and positive ( $\tilde{\nu}_{\text{NCE}} = 10 \text{ cm}^{-1}$ , derived from  $\tilde{\nu}_{\text{iso}} = 1783 \text{ cm}^{-1}$  and  $\tilde{\nu}_{\text{aniso}} = 1793 \text{ cm}^{-1}$ ),<sup>21,35,36</sup> as expected for a highly dipolar liquid;<sup>22–25</sup> (2) for neat DEC, which is less dipolar, the NCE is much smaller ( $\tilde{\nu}_{\text{NCE}} = 3 \text{ cm}^{-1}$ , derived from  $\tilde{\nu}_{\text{iso}} = 1745 \text{ cm}^{-1}$

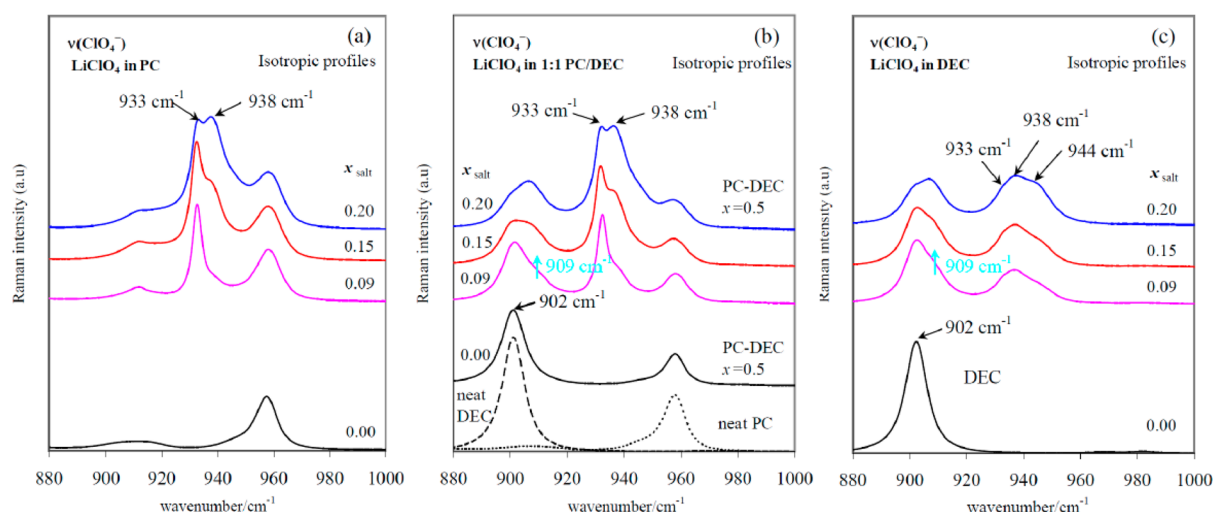


**Figure 3.** Isotropic Raman spectra in the 880–1000  $\text{cm}^{-1}$  spectral region observed for the solutions of  $\text{LiClO}_4$  in (a) liquid PC, (b) equimolar PC/DEC liquid mixture, and (c) liquid DEC, with mole fractions  $x_{\text{salt}} = 0.00, 0.09, 0.15$ , and  $0.20$  (black, pink, red, and blue, respectively). The intensity scales in panels a and b are adjusted so that the intensity of the band of PC at  $850 \text{ cm}^{-1}$  (outside of the frequency region shown here) has the same height.

and  $\tilde{\nu}_{\text{aniso}} = 1748 \text{ cm}^{-1}$ ); and (3) both NCEs are reduced upon 1:1 mixing, but the former is reduced by no more than 50% (to  $8 \text{ cm}^{-1}$ ), as expected for the more dipolar species in a binary mixture.<sup>25,37,38</sup> Upon solvation of  $\text{LiClO}_4$  in liquid PC, rising of a shoulder band is seen in the isotropic Raman spectrum at  $1810 \text{ cm}^{-1}$  (although overlapped with the Fermi resonance band of the neat liquid) and in the anisotropic Raman spectrum at  $1769 \text{ cm}^{-1}$ , as shown in Figure 1a,b, similarly to the case of salt solvation in liquid acetone.<sup>27,28</sup> The NCE of this newly appearing feature (the cluster component band) is large and negative ( $-41 \text{ cm}^{-1}$ ). Upon solvation of  $\text{LiClO}_4$  in liquid DEC, a similar appearance of a new band is clearly seen in the anisotropic Raman spectrum at  $1717 \text{ cm}^{-1}$ , as shown in Figure 1f, but no new band or shoulder is discernible in the isotropic Raman spectrum, as shown in Figure 1e.

To help interpretation of these observations, we may consult (as in the cases of the solutions of alkali or alkaline earth metal salts in liquid acetone<sup>27,28</sup>) the calculation results on cluster species, which are shown in Figure 2. Among the clusters consisting of PC,  $\text{Li}^+$ , and  $\text{ClO}_4^-$ , a large negative NCE ( $>20 \text{ cm}^{-1}$  in magnitude) is calculated for  $(\text{PC})_3\text{Li}^+$ ,  $(\text{PC})_4\text{Li}^+$ , and  $(\text{PC})_3\text{Li}^+\text{ClO}_4^-$ . The observed value of the NCE ( $-41 \text{ cm}^{-1}$ ) is most consistent with  $(\text{PC})_4\text{Li}^+$  (its NCE calculated as  $-35.6 \text{ cm}^{-1}$ ), suggesting the solvation number of  $n = 4$  for the first solvation shell of  $\text{Li}^+$  in liquid PC.<sup>6,12,29,39–42</sup> Similarly, among the clusters consisting of DEC,  $\text{Li}^+$ , and  $\text{ClO}_4^-$ , a large negative NCE is calculated for  $(\text{DEC})_3\text{Li}^+$ ,  $(\text{DEC})_4\text{Li}^+$ , and  $(\text{DEC})_3\text{Li}^+\text{ClO}_4^-$ . Then, the observed spectral features shown in Figure 1e,f would be most reasonably interpreted as indicating the spectral overlap of the cluster component band with the bulk component band at  $1745 \text{ cm}^{-1}$  in the isotropic Raman spectrum. According to this interpretation, the observed value of the NCE of the cluster component band is  $-28 \text{ cm}^{-1}$  and is consistent with either of the three solvation structures (the NCE calculated as  $-23.7$ ,  $-27.1$ , and  $-22.3 \text{ cm}^{-1}$ ). The absence of any spectral feature in the wavenumber region around  $1717 \text{ cm}^{-1}$  in the isotropic Raman spectrum (Figure 1e) denies a solvation structure with a much smaller value of NCE.

Now we turn to the isotropic and anisotropic Raman spectra observed for the solutions of  $\text{LiClO}_4$  in the equimolar PC/DEC mixed solvent, which are shown in Figure 1c,d. Upon solvation of  $\text{LiClO}_4$ , rising of a shoulder band is seen in the isotropic Raman spectrum at  $1811 \text{ cm}^{-1}$  and in the anisotropic Raman spectrum at  $1775 \text{ cm}^{-1}$  in the spectral region nearby the  $\text{C}=\text{O}$  stretching mode of PC, while no new band or shoulder is discernible in the spectral region of the  $\text{C}=\text{O}$  stretching mode of DEC for the concentration range of  $x_{\text{salt}} = 0.00$  to  $0.15$ . The NCE resulting from the bands at  $1811$  and  $1775 \text{ cm}^{-1}$  is  $-36 \text{ cm}^{-1}$ . This value is large and negative but is slightly smaller in magnitude than that observed for the solutions of  $\text{LiClO}_4$  in liquid PC. Consulting the values of NCE calculated for the cluster species shown in Figure 2, this result is interpreted as indicating the solvation structure of  $(\text{PC})_3\text{Li}^+$ ,  $(\text{PC})_3(\text{DEC})_1\text{Li}^+$ , and/or  $(\text{PC})_3\text{Li}^+\text{ClO}_4^-$  (the NCE calculated as  $-22.7$ ,  $-27.1$ , and  $-25.5 \text{ cm}^{-1}$ ) or its mixture with  $(\text{PC})_4\text{Li}^+$ . (These possibilities will be further evaluated later.) In other words, the large magnitude of the negative NCE observed for the cluster component band in the  $1765\text{--}1820 \text{ cm}^{-1}$  spectral region clearly indicates that three or more PC molecules are clustering around the  $\text{Li}^+$  ion in the solutions of  $\text{LiClO}_4$  in the equimolar PC/DEC mixed solvent. In contrast, there is no spectral feature indicating the clustering of three or more DEC molecules around the  $\text{Li}^+$  ion in the same solutions. Therefore, this result suggests the presence of preferential solvation around the  $\text{Li}^+$  ion in the solutions of  $\text{LiClO}_4$  in the equimolar PC/DEC mixed solvent, with a higher population of PC around the ion than in the bulk.

To see whether some DEC molecules are directly interacting with the  $\text{Li}^+$  ion in the solutions and whether the  $\text{ClO}_4^-$  ion forms a contact ion pair with the  $\text{Li}^+$  ion, the profiles of the isotropic Raman spectra are also examined in the spectral region of the OCO bending mode of DEC and the Cl–O symmetric stretching mode of the  $\text{ClO}_4^-$  ion. The results are shown in Figure 3. Inspecting first the OCO bending mode of DEC, which appears at  $902 \text{ cm}^{-1}$  in neat liquid DEC and in the equimolar PC/DEC liquid mixture (Figure 3c,b), the rising of a shoulder band is observed at  $909 \text{ cm}^{-1}$ , which is attributable to the  $\text{C}=\text{O}\cdots\text{Li}^+$  interacting species. This means that some DEC



molecules are interacting with the  $\text{Li}^+$  ion both in the solutions of  $\text{LiClO}_4$  in the equimolar PC/DEC mixed solvent and in the solutions in neat liquid DEC. This interpretation is supported by the calculations on the cluster species of  $(\text{PC})_3(\text{DEC})_1\text{Li}^+$ ,  $(\text{DEC})_3\text{Li}^+$ ,  $(\text{DEC})_4\text{Li}^+$ , and  $(\text{DEC})_3\text{Li}^+\text{ClO}_4^-$  shown in Table 1, which indicate that the OCO bending mode shifts to the

**Table 1. Frequencies of the OCO Bending Mode of Diethyl Carbonate Calculated for an Isolated Molecule and the Molecules in Some Cluster Species<sup>a</sup>**

species	frequency ( $\text{cm}^{-1}$ ) <sup>b</sup>	frequency shift ( $\text{cm}^{-1}$ ) <sup>c</sup>
isolated	897.7	
$(\text{PC})_3(\text{DEC})_1\text{Li}^+$	904.4	6.7
$(\text{DEC})_3\text{Li}^+$	906.2	8.5
$(\text{DEC})_4\text{Li}^+$	901.9	4.2
$(\text{DEC})_3\text{Li}^+\text{ClO}_4^-$	902.5	4.8

<sup>a</sup>Calculated at the B3LYP/6-31+G(2df,p) level, scaled by 0.9860.

<sup>b</sup>Average value is taken for the species with three or four DEC molecules. In those cases, the frequencies of the individual modes are distributed within  $\pm 2 \text{ cm}^{-1}$ . <sup>c</sup>Shift from the frequency of an isolated molecule.

high-wavenumber side by  $4\text{--}9 \text{ cm}^{-1}$  upon  $\text{C}=\text{O}\cdots\text{Li}^+$  complex formation (as compared with an isolated DEC molecule). Inspecting next the spectral features in the region of the  $\text{Cl}\text{--}\text{O}$  symmetric stretching mode of the  $\text{ClO}_4^-$  ion ( $925\text{--}950 \text{ cm}^{-1}$ ), it is seen in Figure 3a,b that a sharp band appears at  $933 \text{ cm}^{-1}$  for  $x_{\text{salt}} = 0.09$ ; then, another band at  $938 \text{ cm}^{-1}$  grows as the concentration increases (with a marginal appearance of a shoulder at  $944 \text{ cm}^{-1}$  for  $x_{\text{salt}} = 0.20$ ) in the cases of the solutions of  $\text{LiClO}_4$  both in liquid PC and in the equimolar PC/DEC mixed solvent, while in the case of the solutions in liquid DEC (Figure 3c) the band is broad and a shoulder is clearly seen at  $944 \text{ cm}^{-1}$ . According to the assignments given in previous studies,<sup>43–46</sup> the bands at  $933$ ,  $938$ , and  $944 \text{ cm}^{-1}$  are assigned to the free ion, solvent-separated ion pair, and contact ion pair, respectively. Then, the observed spectral features mean that the  $\text{ClO}_4^-$  ion is present as a free ion in dilute solutions in PC and PC/DEC and forms a solvent-separated ion pair but not a contact ion pair as the major species as the concentration increases, while it is abundantly present as solvent-separated and contact ion pairs in the solutions in DEC.

For the solutions in liquid PC, this information is consistent with the solvation structure of  $(\text{PC})_4\text{Li}^+$  derived from the NCE in the  $\text{C}=\text{O}$  stretching region. The free ion nature of  $\text{ClO}_4^-$  in PC has also been suggested in previous studies.<sup>47,48</sup> For the solutions in liquid DEC, it is now confirmed that, among the possible solvation structures derived from the NCE, both the  $(\text{DEC})_n\text{Li}^+$  (with  $n = 3$  and/or  $4$ ) and  $(\text{DEC})_3\text{Li}^+\text{ClO}_4^-$  structures are present. In the case of the former, the  $\text{ClO}_4^-$  ion is present outside of the first solvation shell of the  $\text{Li}^+$  ion and forms a solvent-separated ion pair. In contrast, for the solutions in the equimolar PC/DEC mixed solvent, among the possible solvation structures derived from the NCE, the  $(\text{PC})_3\text{Li}^+\text{ClO}_4^-$  structure (with contact ion pairing between  $\text{Li}^+$  and  $\text{ClO}_4^-$ ) is denied by the absence of the  $944 \text{ cm}^{-1}$  band in the spectra shown in Figure 3b. It is most probable that the  $(\text{PC})_3(\text{DEC})_1\text{Li}^+$  structure is abundantly present, because there is a sign indicating the  $\text{C}=\text{O}\cdots\text{Li}^+$  interaction of DEC at  $909 \text{ cm}^{-1}$  in the same spectra as discussed above. The  $(\text{PC})_3\text{Li}^+$  and/or  $(\text{PC})_4\text{Li}^+$  structures may also be present.

In summary, it has been shown that, in the solutions of  $\text{LiClO}_4$  in the equimolar PC/DEC mixed solvent, preferential solvation occurs around the  $\text{Li}^+$  ion, with a higher population of PC around the ion than in the bulk. This property of the solvation structure is derived from the large negative NCE ( $\tilde{\nu}_{\text{NCE}} = -36 \text{ cm}^{-1}$ , obtained from  $\tilde{\nu}_{\text{iso}} = 1811 \text{ cm}^{-1}$  and  $\tilde{\nu}_{\text{aniso}} = 1775 \text{ cm}^{-1}$ ) observed for the cluster component band of the  $\text{C}=\text{O}$  stretching mode shown in Figure 1c,d and its interpretation based on the calculations on some cluster species shown in Figure 2. The most probable solvation structure is  $(\text{PC})_3(\text{DEC})_1\text{Li}^+$ . In other words, the  $\text{Li}^+$  ion is preferentially solvated by PC molecules, totally protected from direct interaction (contact ion pairing) with the  $\text{ClO}_4^-$  ion (as shown by the absence of the  $944 \text{ cm}^{-1}$  band in the spectra shown in Figure 3b), and is supposed to move rather smoothly in the liquid mixture of rather low viscosity (as compared with neat liquid PC). Without the mixing of PC,  $\text{Li}^+$  is not protected from direct interaction with  $\text{ClO}_4^-$  and forms a contact ion pair, as seen in Figure 3c. We expect that the results of the present study can be helpful for a better understanding of the solvation structure around the  $\text{Li}^+$  ion in mixed cyclic/linear carbonate solvents, which is considered to be an important factor for the performance of lithium-based rechargeable batteries.

## ■ ASSOCIATED CONTENT

### § Supporting Information

The Supporting Information is available free of charge on the ACS Publications website at DOI: 10.1021/acs.jpclett.5b01524.

Details of the experimental and computational procedures. (PDF)

## ■ AUTHOR INFORMATION

### Corresponding Authors

\*M.G.G.: E-mail: mariagrazia.giorgini@unibo.it.

\*H.T.: E-mail: torii.hajime@shizuoka.ac.jp.

### Notes

The authors declare no competing financial interest.

## ■ ACKNOWLEDGMENTS

This study was supported in part by a Grant-in-Aid for Scientific Research from the Ministry of Education, Culture, Sports, Science, and Technology of Japan. The Italian Ministry of University and Research is acknowledged for financial support within PRIN 2010-11.

## ■ REFERENCES

- (1) Xu, K. Nonaqueous Liquid Electrolytes for Lithium-Based Rechargeable Batteries. *Chem. Rev.* **2004**, *104*, 4303–4417.
- (2) Baddour-Hadjean, R.; Pereira-Ramos, J.-P. Raman Microspectrometry Applied to the Study of Electrode Materials for Lithium Batteries. *Chem. Rev.* **2010**, *110*, 1278–1319.
- (3) Xu, K. Electrolytes and Interphases in Li-Ion Batteries and Beyond. *Chem. Rev.* **2014**, *114*, 11503–11618.
- (4) Xu, K.; Lam, Y.; Zhang, S. S.; Jow, T. R.; Curtis, T. B. Solvation Sheath of  $\text{Li}^+$  in Nonaqueous Electrolytes and Its Implication of Graphite/Electrolyte Interface Chemistry. *J. Phys. Chem. C* **2007**, *111*, 7411–7421.
- (5) von Wald Cresce, A.; Borodin, O.; Xu, K. Correlating  $\text{Li}^+$  Solvation Sheath Structure with Interphasial Chemistry on Graphite. *J. Phys. Chem. C* **2012**, *116*, 26111–26117.
- (6) Nie, M.; Abraham, D. P.; Seo, D. M.; Chen, Y.; Bose, A.; Lucht, B. L. Role of Solution Structure in Solid Electrolyte Interphase

Formation on Graphite with  $\text{LiPF}_6$  in Propylene Carbonate. *J. Phys. Chem. C* **2013**, *117*, 25381–25389.

(7) von Cresce, A.; Xu, K. Preferential Solvation of  $\text{Li}^+$  Directs Formation of Interphase on Graphitic Anode. *Electrochem. Solid-State Lett.* **2011**, *14*, A154–A156.

(8) Matsuda, Y.; Fukushima, T.; Hashimoto, H.; Arakawa, R. Solvation of Lithium Ions in Mixed Organic Electrolyte Solutions by Electrospray Ionization Mass Spectroscopy. *J. Electrochem. Soc.* **2002**, *149*, A1045–A1048.

(9) Bogle, X.; Vazquez, R.; Greenbaum, S.; von Wald Cresce, A.; Xu, K. Understanding  $\text{Li}^+$ -Solvent Interaction in Nonaqueous Carbonate Electrolytes with  $^{17}\text{O}$  NMR. *J. Phys. Chem. Lett.* **2013**, *4*, 1664–1668.

(10) Yang, L.; Xiao, A.; Lucht, B. L. Investigation of Solvation in Lithium Ion Battery Electrolytes by NMR Spectroscopy. *J. Mol. Liq.* **2010**, *154*, 131–133.

(11) Reddy, V. P.; Smart, M. C.; Chin, K. B.; Ratnakumar, B. V.; Surampudi, S.; Hu, J.; Yan, P.; Surya Prakash, G. K. NMR Spectroscopic, CV, and Conductivity Studies of Propylene Carbonate-Based Electrolytes Containing Various Lithium Salts. *Electrochem. Solid-State Lett.* **2005**, *8*, A294–A298.

(12) Ong, M. T.; Verners, O.; Draeger, E. W.; van Duin, A. C. T.; Lordi, V.; Pask, J. E. Lithium Ion Solvation and Diffusion in Bulk Organic Electrolytes from First-Principles and Classical Reactive Molecular Dynamics. *J. Phys. Chem. B* **2015**, *119*, 1535–1545.

(13) Postupna, O. O.; Kolesnik, Y. V.; Kalugin, O. N.; Prezhdo, O. V. Microscopic Structure and Dynamics of  $\text{LiBF}_4$  Solutions in Cyclic and Linear Carbonates. *J. Phys. Chem. B* **2011**, *115*, 14563–14571.

(14) Skarmoutsos, I.; Ponnuchamy, V.; Vetere, V.; Mossa, S.  $\text{Li}^+$  Solvation in Pure, Binary, and Ternary Mixtures of Organic Carbonate Electrolytes. *J. Phys. Chem. C* **2015**, *119*, 4502–4515.

(15) Borodin, O.; Smith, G. D. Quantum Chemistry and Molecular Dynamics Simulation Study of Dimethyl Carbonate: Ethylene Carbonate Electrolytes Doped with  $\text{LiPF}_6$ . *J. Phys. Chem. B* **2009**, *113*, 1763–1776.

(16) Xu, K.; von Wald Cresce, A.  $\text{Li}^+$ -Solvation/Desolvation Dictates Interphasial Processes on Graphitic Anode in Li Ion Cells. *J. Mater. Res.* **2012**, *27*, 2327–2341.

(17) Wang, J.; Wu, Y.; Xuan, X.; Wang, H. Ion–Molecule Interactions in Solutions of Lithium Perchlorate in Propylene Carbonate + Diethyl Carbonate Mixtures: An IR and Molecular Orbital Study. *Spectrochim. Acta, Part A* **2002**, *58*, 2097–2104.

(18) Morita, M.; Asai, Y.; Yoshimoto, N.; Ishikawa, M. A Raman Spectroscopic Study of Organic Electrolyte Solutions Based on Binary Solvent Systems of Ethylene Carbonate with Low Viscosity Solvents which Dissolve Different Lithium Salts. *J. Chem. Soc., Faraday Trans.* **1998**, *94*, 3451–3456.

(19) Klassen, B.; Aroca, R.; Nazri, M.; Nazri, G. A. Raman Spectra and Transport Properties of Lithium Perchlorate in Ethylene Carbonate Based Binary Solvent Systems for Lithium Batteries. *J. Phys. Chem. B* **1998**, *102*, 4795–4801.

(20) Castriota, M.; Cazzanelli, E.; Nicotera, I.; Coppola, L.; Oliviero, C.; Ranieri, G. A. Temperature Dependence of Lithium Ion Solvation in Ethylene Carbonate– $\text{LiClO}_4$  Solutions. *J. Chem. Phys.* **2003**, *118*, 5537–5541.

(21) Fini, G.; Mirone, P.; Fortunato, B. Evidence for Short-Range Orientation Effects in Dipolar Aprotic Liquids from Vibrational Spectroscopy. Part 1.—Ethylene and Propylene Carbonates. *J. Chem. Soc., Faraday Trans. 2* **1973**, *69*, 1243–1248.

(22) Logan, D. E. The Non-Coincidence Effect in the Raman Spectra of Polar Liquids. *Chem. Phys.* **1986**, *103*, 215–225.

(23) Torii, H.; Tasumi, M. Local Order and Transition Dipole Coupling in Liquid Methanol and Acetone as the Origin of the Raman Noncoincidence Effect. *J. Chem. Phys.* **1993**, *99*, 8459–8465.

(24) Torii, H. Computational Methods for Analyzing the Intermolecular Resonant Vibrational Interactions in Liquids and the Noncoincidence Effect of Vibrational Spectra. In *Novel Approaches to the Structure and Dynamics of Liquids: Experiments, Theories and Simulations*; Samios, J., Durov, V. A., Eds.; Kluwer: Dordrecht, The Netherlands, 2004; pp 343–360.

(25) Giorgini, M. G. Raman Noncoincidence Effect: A Spectroscopic Manifestation of the Intermolecular Vibrational Coupling in Dipolar Molecular Liquids. *Pure Appl. Chem.* **2004**, *76*, 157–169.

(26) Musso, M.; Torii, H.; Ottaviani, P.; Asenbaum, A.; Giorgini, M. G. Noncoincidence Effect of Vibrational Bands in Methanol/ $\text{CCl}_4$  Mixtures and Its Relation to Concentration-Dependent Liquid Structures. *J. Phys. Chem. A* **2002**, *106*, 10152–10161.

(27) Giorgini, M. G.; Torii, H.; Musso, M.; Venditti, G. Influence of Ions on the Structural Organization of Dipolar Liquids Probed by the Noncoincidence Effect: Experimental and Quantum Chemical Results. *J. Phys. Chem. B* **2008**, *112*, 7506–7514.

(28) Giorgini, M. G.; Torii, H.; Musso, M. The Influence of Alkaline Earth Ions on the Structural Organization of Acetone Probed by the Noncoincidence Effect of the  $\nu(\text{C}=\text{O})$  Band: Experimental and Quantum Chemical Results. *Phys. Chem. Chem. Phys.* **2010**, *12*, 183–192.

(29) Hyodo, S.; Okabayashi, K. Raman Intensity Study of Local Structure in Non-Aqueous Electrolyte Solutions—I. Cation–Solvent Interaction in  $\text{LiClO}_4$ /Ethylene Carbonate. *Electrochim. Acta* **1989**, *34*, 1551–1556.

(30) Gorobets, M. I.; Ataev, M. B.; Gafurov, M. M.; Kirillov, S. A. Raman Study of Solvation in Solutions of Lithium Salts in Dimethyl Sulfoxide, Propylene Carbonate and Dimethyl Carbonate. *J. Mol. Liq.* **2015**, *205*, 98–109.

(31) Allen, J. L.; Borodin, O.; Seo, D. M.; Henderson, W. A. Combined Quantum Chemical/Raman Spectroscopic Analyses of  $\text{Li}^+$  Cation Solvation: Cyclic Carbonate Solvents – Ethylene Carbonate and Propylene Carbonate. *J. Power Sources* **2014**, *267*, 821–830.

(32) Barthel, J.; Buchner, R.; Wismeth, E. FTIR Spectroscopy of Ion Solvation of  $\text{LiClO}_4$  and  $\text{LiSCN}$  in Acetonitrile, Benzonitrile, and Propylene Carbonate. *J. Solution Chem.* **2000**, *29*, 937–954.

(33) Seo, D. M.; Reininger, S.; Kutcher, M.; Redmond, K.; Euler, W. B.; Lucht, B. L. Role of Mixed Solvation and Ion Pairing in the Solution Structure of Lithium Ion Battery Electrolytes. *J. Phys. Chem. C* **2015**, *119*, 14038–14046.

(34) Frisch, M. J.; Trucks, G. W.; Schlegel, H. B.; Scuseria, G. E.; Robb, M. A.; Cheeseman, J. R.; Montgomery, J. A., Jr.; Vreven, T.; Kudin, K. N.; Burant, J. C.; et al. *Gaussian 03*, revision D.01; Gaussian, Inc.: Wallingford, CT, 2004.

(35) Brodin, A.; Jacobsson, P. Dipolar Interaction and Molecular Ordering in Liquid Propylene Carbonate: Anomalous Dielectric Susceptibility and Raman Non-Coincidence Effect. *J. Mol. Liq.* **2011**, *164*, 17–21.

(36) Sun, T. F.; Chan, J. B.; Wallen, S. L.; Jonas, J. Raman Noncoincidence Effect of the Carbonyl Stretching Mode in Compressed Liquid Cyclic Carbonates. *J. Chem. Phys.* **1991**, *94*, 7486–7493.

(37) Logan, D. E. The Raman Noncoincidence Effect in Dipolar Binary Mixtures. *Chem. Phys.* **1989**, *131*, 199–207.

(38) Musso, M.; Giorgini, M. G.; Torii, H.; Dorka, R.; Schiel, D.; Asenbaum, A.; Keutel, D.; Oehme, K.-L. The Raman Non-Coincidence Effect of the  $^{12}\text{C}=\text{O}$  Stretching Mode of Liquid Acetone in Chemical and in Isotopic Mixtures. *J. Mol. Liq.* **2006**, *125*, 115–122.

(39) Smith, J. W.; Lam, R. K.; Sheardy, A. T.; Shih, O.; Rizzuto, A. M.; Borodin, O.; Harris, S. J.; Prendergast, D.; Saykally, R. J. X-Ray Absorption Spectroscopy of  $\text{LiBF}_4$  in Propylene Carbonate: A Model Lithium Ion Battery Electrolyte. *Phys. Chem. Chem. Phys.* **2014**, *16*, 23568–23575.

(40) Ganesh, P.; Jiang, D.; Kent, P. R. C. Accurate Static and Dynamic Properties of Liquid Electrolytes for Li-Ion Batteries from ab initio Molecular Dynamics. *J. Phys. Chem. B* **2011**, *115*, 3085–3090.

(41) Kameda, Y.; Umebayashi, Y.; Takeuchi, M.; Wahab, M. A.; Fukuda, S.; Ishiguro, S.; Sasaki, M.; Amo, Y.; Usuki, T. Solvation Structure of  $\text{Li}^+$  in Concentrated  $\text{LiPF}_6$ -Propylene Carbonate Solutions. *J. Phys. Chem. B* **2007**, *111*, 6104–6109.

(42) Masia, M.; Probst, M.; Rey, R. Ethylene Carbonate– $\text{Li}^+$ : A Theoretical Study of Structural and Vibrational Properties in Gas and Liquid Phases. *J. Phys. Chem. B* **2004**, *108*, 2016–2027.

- (43) Klassen, B.; Aroca, R.; Nazri, G. A. Lithium Perchlorate: Ab Initio Study of the Structural and Spectral Changes Associated with Ion Pairing. *J. Phys. Chem.* **1996**, *100*, 9334–9338.
- (44) Battisti, D.; Nazri, G. A.; Klassen, B.; Aroca, R. Vibrational Studies of Lithium Perchlorate in Propylene Carbonate Solutions. *J. Phys. Chem.* **1993**, *97*, 5826–5830.
- (45) Frost, R. L.; James, D. W.; Appleby, R.; Mayes, R. E. Ion-Pair Formation and Anion Relaxation in Aqueous Solutions of Group 1 Perchlorates. A Raman Spectral Study. *J. Phys. Chem.* **1982**, *86*, 3840–3845.
- (46) James, D. W.; Mayes, R. E. Ion–Ion–Solvent Interactions in Solution. I. Solutions of  $\text{LiClO}_4$  in Acetone. *Aust. J. Chem.* **1982**, *35*, 1775–1784.
- (47) Sagane, F.; Abe, T.; Ogumi, Z.  $\text{Li}^+$ -Ion Transfer through the Interface between  $\text{Li}^+$ -Ion Conductive Ceramic Electrolyte and  $\text{Li}^+$ -Ion-Concentrated Propylene Carbonate Solution. *J. Phys. Chem. C* **2009**, *113*, 20135–20138.
- (48) Kondo, K.; Sano, M.; Hiwara, A.; Omi, T.; Fujita, M.; Kuwae, A.; Iida, M.; Mogi, K.; Yokoyama, H. Conductivity and Solvation of  $\text{Li}^+$  Ions of  $\text{LiPF}_6$  in Propylene Carbonate Solutions. *J. Phys. Chem. B* **2000**, *104*, 5040–5044.